J Korean Soc Appl Biol Chem (2013) 56, 533–540
DOI 10.1007/s13765-013-3167-9

ORIGINAL ARTICLE

The Potential Restorative Effects of Strontium-doped Bioactive Glass on Bone Microarchitecture after Estrogen-deficieny Induced Osteoporosis: Physico-chemical and Histomorphometric Analyses

Samira Jebahi · Hassane Oudadesse · Jiheun Elleuch · Slim Tounsi · Hassib Keskes · Pascal pellen · Tarek Rebai · Abdelfatteh El Feki · Hafed El Feki

Received: 13 July 2013 / Accepted: 22 August 2013 / Published Online: 31 October 2013

Abstract Strontium (Sr) compounds have become increasingly popular in the field of osteoporosis treatment. However, the quality of new bone after implantation of strontium-containing bioceramics has yet to be investigated. In the present study, the newly formed bone tissue around strontium-doped bioactive glass (BG-Sr) implants was characterized. BG-Sr was implanted in the femoral condyl of ovariectomised rats (OVX). The resected bone was prepared for analysis using several physico-chemical and biological assays such as Fourier transform infrared spectroscopy, X-ray diffraction, scanning electron microscopy, energy-dispersive X-ray, and histomorphometry. BG-Sr biomaterial favored calcium phosphate layer integration on the surface of the glass and offered better bioactivity. Moreover, the histomorphometric analysis demonstrated that BV/TV, N. Ob were significantly higher in BG-Sr treated rats groups than those of BG groups. However, Ob. S/ BS, and OV/BV were significantly lower in BG-Sr treated rats groups than those of BG groups. The (Oc.S/ BS) was significantly decreased in BG-Sr groups, when compared with that of BG rat groups. On the other hand, the MS/BS had not significantly decreased in the BG-Sr treated rats groups when compared with that of BG groups, however; it was significantly higher when compared with control and OVX groups. These findings suggest that BG-Sr can be used as an inhibitory therapeutic potential of osteoporosis by delivering strontium to stimulate new bone remodeling.

Keywords bioactive glass · bone regeneration · ions release · osteoporosis · strontium effect

S. Jebahi (✉) · H. Oudadesse · P. pellen
University of Rennes 1, UMR CNRS 6226, Campus de Beaulieu, 263 av. du Général Leclerc, 35042 Rennes, France
E-mail: jebahisamira@yahoo.fr

S. Jebahi · A. El Feki
Animal Ecophysiology Laboratory, Sfax Faculty of Science, Department of Life Sciences , Sfax ,Tunisia

H. El Feki
Science Materials and Environement laboratory, Sfax Faculty of Science , Sfax, Tunisia.

H. Keskes · T. Rebai
Histology,Orthopaedic and Traumatology laboratory, Sfax Faculty of Medicine, Sfax ,Tunisia

J. Elleuch · S. Tounsi
Laboratory of Biopesticides, Centre of Biotechnology of Sfax, P.O.Box K. 3038. Sfax, Tunisia

Introduction

The fast development of bioactive materials for hard tissue replacement allowed significant advances in the skin, bone, maxillofacial and craniofacial surgeries (Nguyen et al., 2010; Lochman et al., 2011). Bioactive materials serve as an implant that enhances healing and bone tissue regeneration in osteoporotic fractures. It has become widespread, especially when clinical experiments show that the conventional metal reinforcement method for fractured bone is not practical because of bone fragility. These materials exhibit reactive surfaces able to bond to living tissues and to produce nucleation and growth of an apatite-like phase at the implant-tissue interface. Among these materials, bioactive glass has been extensively used in biomaterials science applications (Lusvardi et al., 2008). It has been proposed as an excellent candidate for local drug delivery (Lakhkar et al., 2011) and bone tissue regeneration (Gorustovich et al., 2010). The addition of factors, molecules and ions to bioactive glass, which

stimulate cell differentiation and proliferation, has recently presented to bioactive glass an advance in the field of implantology.

Sr, a naturally occurring trace element, was recently suggested as treatment modality for osteoporosis; owing to its both antiresorptive and anabolic effects (Isaac et al., 2011, Jebahi et al., 2012). Sr is incorporated into bone by two mechanisms: (a) surface exchange involving the incorporation of Sr into the crystal lattice of the bone mineral and (b) ionic substitution whereby Sr is taken up by ionic exchange with bone calcium (Ca). In addition to the chemical reactions on the bioactive glass surface leading to bone bonding, recent studies have proven that ion dissolution released from bioactive glass can activate gene expression in osteoprogenitor cells and give rise to enhanced bone regeneration (Pan et al., 2010).

The bone-bonding potentiality of a biomaterial is often estimated by examining its ability of an apatite layer to form on its surface after immersion in a simulated body fluid (SBF). However, the validity of this method for evaluating bone-bonding ability has not been assessed systematically. Therefore, the SBF carbonate content can vary during the test, which consequently affects the pH. Moreover, no organic molecules are present, such as proteins, which are known to be apatite nucleation inhibitors *in vivo* (Bohner et al., 2009). The test can produce false positive results; for example, calcium sulphate forms apatite in SBF to be bioactive, while it resorbs too rapidly *in vivo* (Kokubo et al., 2006). The test can produce false negative results; for example, the test does not call for mechanical agitation of the solution. The SBF test is useful as an initial *in vitro* test, but promising materials should be followed up with *in vitro* cells and *in vivo* animal studies. *In vitro* study, in the presence of saos2 cells, the introduction of Sr at 0.1 wt % induces cells proliferation at about 14.3% (Oudadesse et al., 2011).

Here, the evidence of the beneficial effects of Sr on bone growth motivated us to incorporate this chemical element, in trace amount in the ceramic SiO_2-CaO-Na_2O-P_2O_5 system for skeletal tissue applications. After its implantation in ovareiectomized rat, this work aimed to study the influence of incorporated strontium bioactive glass activities to investigate both its degradation and biocompatibility behavior. Therefore, the study evaluations are based on physico-chemical analyses, conventional histology and histomorphometry.

Material and methods

Bioactive glass synthesis. The first studied composition was pure 46S6 possessing a composition closes to that of Hench's 45S5 (Hench et al., 1998). Moreover, it was used as a reference composition to evaluate our experimental procedure. Then, a percentage of 0.1% wt of Sr was introduced to the 46S6 bioactive glass. This content of Sr is close to that of the human bone. Appropriate amounts of calcium metasilicate, sodium metasilicate, sodium metaphosphate, and magnesium oxide were weighed and mixed for 45 min using a planetary mixer. The powdered mixture was heated in a platinum crucible at 1300°C for 3 h. The molten material was then poured into preheated brass molds, in order to form BG-Sr cylinders of 13 mm in diameter and 10 mm in height. The prepared samples were annealed at the appropriate temperature in 4 h, corresponding to the phase transition temperature of the glass composition (about 560°C), in a regulated muffle furnace. The muffle furnace was cooled to room temperature at a rate of 1°C min^{-1} (Oudadesse et al., 2011). After elaboration, the powder particles sized between 40–63 μm were compressed in a perfectly isostatic manner. The prepared implants were sterilized by γ-irradiation from a 60 Co Source gamma irradiation, at a dose of 25 Gy (Equinox, UK), using standard procedures for medical devices.

Animal model. Female Wistar rats (16–9 weeks of age), obtained from the central pharmacy, Tunisia and bred in the central animal house were used in this study. The rats were acclimatized to their new environment during 7 days before the commencement of the study. The animals were fed on a pellet diet (Sicco, Tunisia) and water *ad libitum*. All the animals were kept under climate-controlled conditions (25°C, 55% humidity and 12 h of light alternating with 12 h of darkness). The handling of the animals was approved by the Tunisian ethical committee for the care and use of laboratory animals. All rats were randomly divided into four groups (5 animals per group): the first group (I): used as negative control (CT). Sixty days after bilateral ovariectomy, Group II, III and IV used respectively as positive control (OVX), implanted with BG (OVX -BG) , BG-Sr (OVX -BG-Sr).

Surgical and postoperative protocol. All surgical interventions were performed in aseptic conditions under general anesthesia. Anaesthesia was induced with xylazine (7 to 10 mg/kg (i.P) ROMPUN® 2%) and ketamine (70 to 100 mg/kg (I.M.) imalgene®) depending on the body weight. The pre-operative preparation of the surgical sites was routinely carried out; by cleaning it with 96% alcohol and antiseptic solutions (PROLABO; AnalaR Normapur®, France). The resulting bone defects were irrigated profusely with physiological saline solution (0.9 wt. % NaCl; Ref.091214; Siphal, Tunisia) to eliminate bone debris. A drilled bone hole; of 3-mm diameter and 4-mm deep, was created on the lateral aspect of the femoral condyle using a refrigerated drill to avoid heat generation and subsequent bone necrosis. The drill-hole was filled with 10mg of BG-Sr in OVX -BG-Sr group and with 10mg of BG in OVX -BG group. After implant insertion, on the 4^{th}, 7^{th}, 15^{th}, 30^{th}, 60^{th} and 90^{th} days, all rats were sacrificed and specimens were harvested for biological and physico-chemical evaluation.

Physicochemical analyses. Identification of chemical groups of the implant on the 4^{th}, 7^{th}, 15^{th}, 30^{th} and 60^{th} days were carried out by IR spectroscopy (FTIR) (Bruker Equinox 55). Investigations were performed in the absorbance mode, using KBr pellet technique, at 4 cm^{-1} resolution. Spectra were analysed in the range of 400 and 400 cm^{-1} wave length. Moreover, X-ray diffraction (XRD) technique (Philips PW 3710 diffractometer) allowed us to

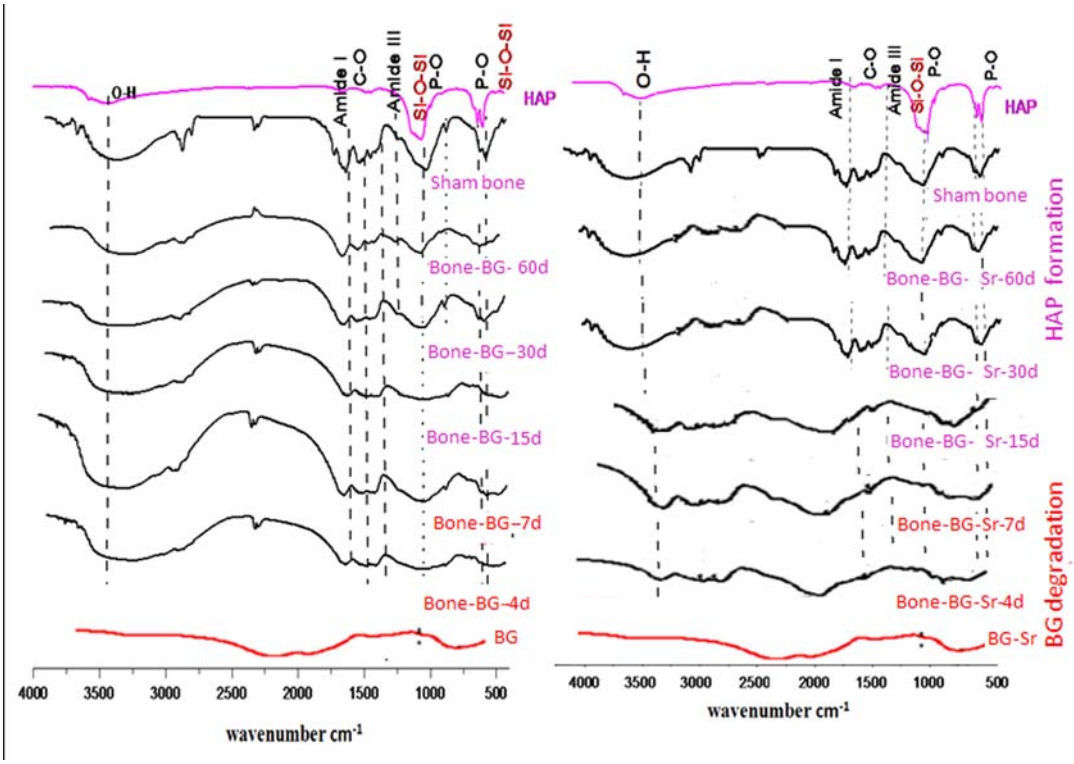

Fig. 1 Infrared spectra from bones implanted by bioactive glass (BG) (A) and bioactive glass doped strontium (BG-Sr) (B) after 4, 7, 15, 30, and 60 days compared to hydroxyapatite (HA) as reference spectrum. Infrared spectra comparison between bones implanted by BG-Sr and BG after 30 days of implantation compared to hydroxyapatite reference spectrum(C).

verify the progressive healing of implanted bone. The semi-quantitative chemical analysis was performed by EDS on BG-Sr and BG-bone covered with a thin film gold-palladium in order to prevent charge accumulation on the surface of the analyzed material.

Histomorphometric evaluation. The implanted femoral condyles were harvested, fixed in Burdack (formalin) and refrigerated. Specimens were dehydrated, using alcohol titrated solutions from 70 to 100% EtOH. Then, the specimens were infiltrated by methylmethacrylate that was allowed to polymerize, before placing it in a mixture of methylmethacrylate and glycolmethacrylate, without prior decalcification. Using a sliding microtome (Reichert-Jung), sections of 6 to 7 μm thick were debited by cutting along a transverse plane. Moreover, the sections were stained with modified Goldner trichrome, toluidine Blue. Bone/Tissue Volume (BV/TV, expressed in %), Osteoid/Bone Surface (OV/BV expressed in %), Bone/Tissue Volume (BV/TV, expressed in %), Osteoid/Bone Surface (OV/BV expressed in %), Osteoclast /Bone Surface (Oc.S/BS, expressed in %), Osteoblast/Bone Surface (Ob.S/BS, expressed in %), Osteoblast Number (N.Ob expressed in mm^{-2}) and Mineralizing Surface (MS/BS) were measured by a point count method (Schenk et al. 1969) using a 25-point integrating filter.

Statistical analysis. The statistical analysis of the data was calculated using Student's t-test. The number of samples, (n) value was 5 animals per group. All values were expressed as means ± SE (standard error) where the significance level was $2\alpha = 0.05$.

Results

General features and behavior of bone. No complication was reported in bone defects during surgeries or postoperatively, which confirmed absence of failure in all implantation sites along the whole study. Moreover, 60 days after surgery, there was no observed macroscopic or microscopic sign of inflammation, directly related to the implanted materials.

FT-IR characterization of specimens "after *in vivo* tests". The characteristic FTIR bands associated with BG-Sr-bone are located at 932 and 1036 cm^{-1}, arising from (Si-O-Si) groups (Fig. 1). 30 days after surgery, those absorbance bands characteristic of the BG-Sr matrix is seemed to disappear and to be masked by the overlapping band of the apatite matrix. Actually, those bands were replaced by 601 cm^{-1} and 564 cm^{-1} (P-O) groups arising from that of the bone-apatite. Therefore, FTIR was used to monitor and compare the formation and the growth of the Ca-P layer in BG-Sr-bone and BG-bone, by detecting the characteristic vibration modes of the P-O and P=O bonds. Moreover, the bands attributed to Ca-P layer were more accentuated in BG-Sr bone Compared to that of the BG, especially after 30 days of implantation. Absorption

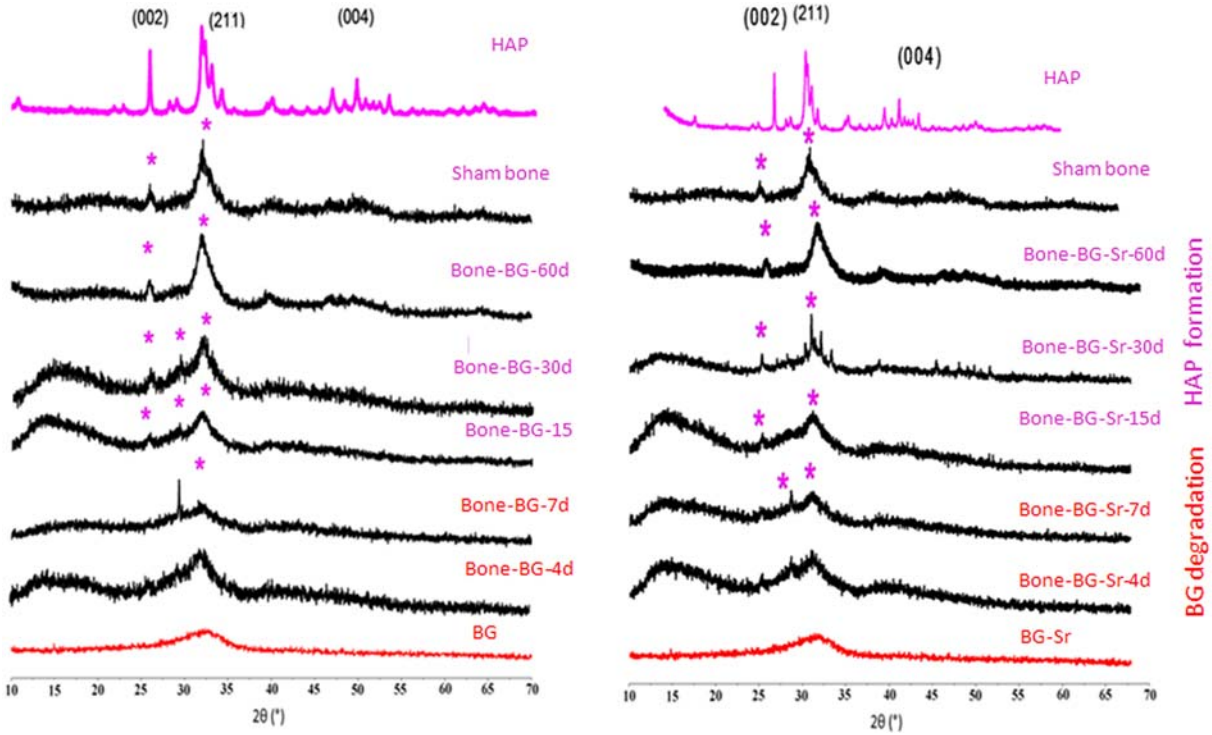

Fig. 2 X-ray Diffraction from bones implanted by bioactive glass (BG) (A) and bioactive glass doped strontium (BG-Sr) (B) after 4, 7, 15, 30 and 60 days compared to hydroxyapatite reference spectrum.

band at 1650 cm^{-1} that was attributed to the stretching (amide I) was also identified. Generally, amide I bands originated from the (C=O) stretching vibrations coupled with the (N-H) bending vibrations (Barth et al. 2002). Moreover, at 1542 cm^{-1} a band (amide II) aroused from the combination of the C-N stretching and the N-H bending vibrations of the bone protein, which might be related to protein matrix formation of implanted bone.

X-ray Diffraction characterization of specimens "after *in vivo* tests". According to the kinetic data in BG-Sr-bone (Fig. 2), we noted a decrease in the relative intensity of peaks 2θ=32°; noting the progressive degradation of the BG-Sr matrix. The diffraction peaks namely at 2θ were 30.2°, 37.1°, 46.6°, 54.8°, 58.2° and 62.7°, corresponded to the most intense characteristic peaks of (Hydroxyapatite) HA that were respectively assigned to the observed following Miller plans: (0 0 2), (2 1 1), (3 1 0), (2 2 2), (1 2 3) and (0 0 4) (Danilchenko et al., 2002). The peaks demonstrated the presence of some biologic apatite characteristic peaks and some neighboring positions of glass ceramic. The glass formed Ca-P-rich layer on its surface and bonded tightly to the living bone. Such peaks, when compared with BG, showed only slight broadening of the mentioned (211) peak. However, after 60 days of surgery, no peak detection from the bioactive glass, which might be attributed to the low content of BG-Sr. Moreover, the absence of the diffraction lines might also be due to the deterioration of the crystal lattice of BG-Sr. At the end of experiment, significant similarity between BG-Sr and the shamed bone was noticed.

Energy Dispersive Spectroscopy (EDS): interface bone-biomaterial mapping. The chemical variation presented in BG-Sr interface after 30 days was 50.8±0.4% for the Ca content and 30.4±0.3% for the P content. Furthermore, the BG interface showed 49.90±0.4% of Ca and 30.60±0.2% of P. BG-Sr presented Ca/P (1.67) ratio while BG exhibited (1.63) for Ca/P ratio. Moreover, after 60 days, poor Si quantities of 4.08±0.03% and 3.78±0.04% were always observed at the interface, of the BG-Sr-bone and BG-bone respectively (Figs. 3A and B). The element maps showed the spatial distribution of Ca, P and Si elements in BG-Sr and BG implant as a function of time (Figs. 3C, D, and E).Moreover it exhibited the presence of small quantity of S 5.09 and 7.6 % of Mg in BG-Sr groups.

Histological analysis. SEM analysis showed the synchronization of bioactive glass degradation and its replacement by natural tissue produced by cells. Actually, the osteoblasts attained a flat morphology and adhered onto the substrate (Figs. 4A, B, C, D and E). Moreover, we noted the presence of HA nodules on the surfaces with an increased thickness of 0.5 µm (Fig. 4F). After 15 days of the surgery, almost all the discs were peripherally and centrally filled with either fibrovascular or osseous tissue. Furthermore, medullary space contained marrow element with few fat cells and fair number of blood vessels could be seen (Figs. 4G and H). Therefore, woven bone progressively had been transformed into mature bone in contact with both BG-Sr and BG

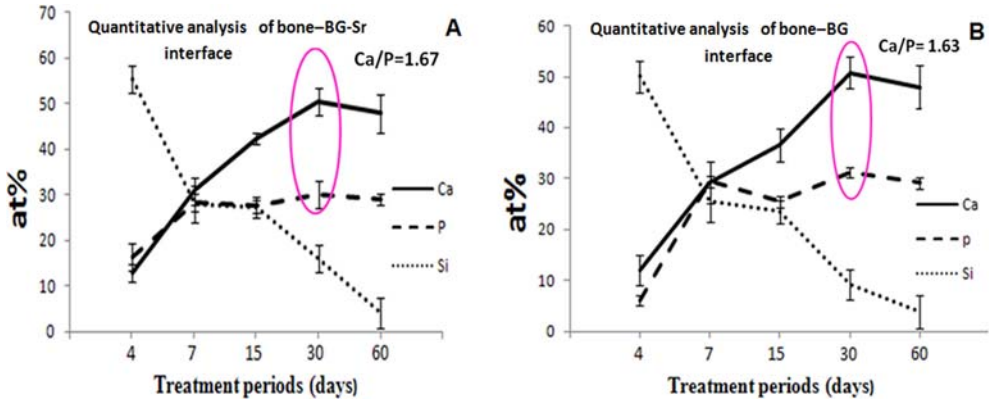

Fig. 3 Ca/P and Si molar ratio (EDS) obtained from the chemical analysis of implanted femoral condyle with bioactive glass (BG) (A) and bioactive glass doped strontium (BG-Sr) biomaterials after 4,7,15,30 and 60 days (B). Energy Dispersive X-ray (EDS) and elemental mapping of Ca, P and Si in bioactive glass doped strontium (BG-Sr-bone) boundary after 4(C), 30(D) and 60 days (E). (Arrows indicate biomaterials and * indicates bone.

(Fig. 4I). Moreover, bone remodeling had reorganized the architecture of the connecting and remaining biomaterial resulting in osteointegration (Fig. 4J). Osteoclasts appeared in a Howship's lacunae-like structure formed in the bone matrix (Fig. 4K). After 60 days of the surgery, there were no signs of inflammation or necrosis (Fig. 4L).

Histomorphometric analysis. After 90-day of the surgery, the quantitative analysis demonstrated that BV/TV, N. Ob and Ob. S/BS were significantly higher in BG-Sr treated rats groups than those of BG groups (Fig. 5A, B, and C). However, the OV/BV was significantly lower in BG-Sr treated rats groups than that of BG groups (Fig. 5D), the (Oc.S/BS) was significantly decreased in BG-Sr groups, when compared with that of BG rat groups (Fig. 5E). On the other hand, the MS/BS had not significantly decreased in the BG-Sr treated rats groups when compared with that of BG groups, however; it was significantly higher when compared with CT and OVX groups (Fig. 5F).

Discussion

Currently, different researches are using diverse types of biomaterial for their application in tissue engineering. Recent studies demonstrated that bioglass can be considered as a promising way of promoting tissue repair. In the present study, the biological performance of pure and Sr doped glasses, with particle size ranging from 40 to 63 ìm, were evaluated *in vivo* for treating osteoporosis induced by castration in rat model.

Owing to its potential bioactivity, the BG-Sr integrated to carbonated hydroxyapatite (CHA) layer when immersed in SBF solution (Oudadesse et al., 2011). In the present *in vivo* study, the bioactivity of the BG-Sr was also confirmed by CHA formation after bioactive glass conversion. In the first 4 days, the XRD pattern of the as-prepared BG-Sr and BG showed broad peaks typical to an amorphous glass. Comparison between BG-Sr and BG degradation indicated that while a CHA layer was formed in both cases, the degradation and conversion of the BG-Sr glass were more enhanced *in vivo*, than those of the BG biomaterial. Moreover, 30 days later, the XRD peaks of CHA layer on the BG-Sr-bone was indicating more intense better bioactivity and consequence of the more 'dynamic' system existing *in vivo* (Zhang et al. 2010) when compared with those of BG bone. That difference in XRD peak intensity might be due to the introduction of Sr in the initial BG amount. On the other hand, Sr can regulated both mRNA and protein levels of osteoblasts, induced signals for osteoclastogenesis, had positive effects on osteoblastic replication, differentiation and lifespan (Zhu et al., 2007) and accentuated the bone formation.

The bioactivity of the biomaterials *in vivo* induced dissolution of the network modifiers and led to the selective release of ions (Jallot et al., 2000). Furthermore, sodium and potassium were rapidly exchanged with the surrounding implants and then Silicon was released. Moreover, calcium and phosphorus were released at slower rate from the glass, which led to the CHA formation on the surface of biomaterials as demonstrated by SEM analyses. Moreover, 60 days after implantation, the peaks corresponding to those of HA as reference were compared to the pattern of the trabecullar bone. They showed broader and less intense peaks, indicating the formation of a poorly crystallized CHA layer.

FTIR spectra of BG and BG-Sr-bone showed slight decrease in the labile PO_4^{3-} at 610 cm^{-1} that might reflect in part an interaction between the Ca and P crystals and specific constituents of the Sr incorporation in the lattice structure (De Carmejane et al., 2005). When we compared the variations in FTIR-derived values measured in BG and BG-Sr, we noted low-turnover of samples on the days 4 and 7, which were characterized by reduced formative CHA activity, with reduced resorptive activity as well. Therefore, those phenomena could be due to the failure to maintain an appropriate bone matrix. In fact, healing of osteoporotic bone was characterized by a reduced metabolic state leading to the formation of few new crystals (Young-Su et al., 2012). Moreover, the Si peak about 460 cm^{-1} was still broad,

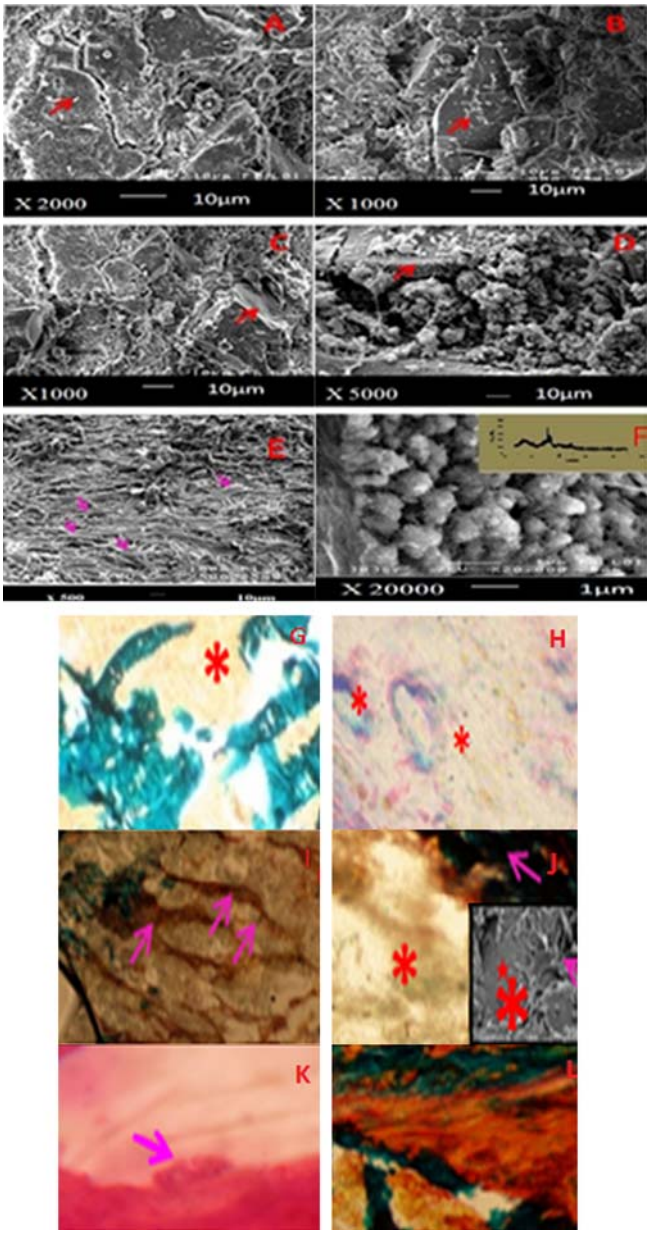

Fig. 4 SEM image of *in vivo* biodegradation bioactive glass behavior (BG) (A, B) and (C, D) bioactive glass doped strontium BG-Sr in the femoral condyle of overictomized female Wistar rats. Arrows indicate break-down of bioactive glass (BG) into particles. Hydroxyapatite (CHA) nodules formation as an indicator of deposition of mineral from environment in contact with bioactive glass doped strontium (BG-Sr) after 30 days of implantation superposed by X-ray Diffraction (E). Well-organized cells had long extensions and appeared to be flat and well spread like in cell culture media (F). Marrow element ×40 (G). Sections of blood vessels ×100 (H). Layer of woven bone ×40 (I). Osteointegration BG-Sr and bone ×40 (asterisk indicates BG-Sr, arrow indicates bone) (J). Osteoclasts appeared in a Hawship's lacunae-formed on BG-Sr biomaterial (asterisk indicates BG-Sr, arrow indicates osteoclast) ×100 (K). 60 days after surgery, osseointegration of bone without any inflammation or necrosis x 40 (Fig.L). Goldner's trichrome staining (G, I, J, L), Toluidine Blue staining (H, K).

indicating that the CHA layer was thin or possibly discontinuous. However, the high turnover in the second period of 15 and 30 days, faster bioactivity of BG-Sr compared to BG that was highlighted by faster decrease of the bands corresponding to bioactive glass and gradual replacement by bone tissue.

Approximately after 2 weeks, SEM analyses showed fissures appeared in bioactive glass. It has been postulated that osteoprogenitor cells enter those cracks and differentiate into osteoblasts (Furusawa et al., 1997; Furusawa et al., 1998; Wiesmann et al., 2004; Wahl et al., 2006). Bioactive glass biodegradation can proceed either by osteoclastic activity or chemical dissolution by tissue fluids (hydrolytic degradation) (Da Cruz et al., 2008). In this study, 90 days after surgery, 0.1 W% Sr stimulated bone formation without altering bone mineralization. In fact, there were no signs of excessive mineralization or other detrimental alterations of the mineralized bone matrix. Furthermore, the significant increase in N.Ob and Ob.S/BS in BG-Sr treated rats groups as compared with those of BG groups was a confirmation of newly produced bone tissue, faced with persisting bone resorption. Those findings were supported by a concomitant increase in BV/TV, which was confirmed by significant increase in OV/BV on the 90th day after surgery as compared to the control group. That augmentation parameter was not an indicator of a mineralization defect, because all values were evidently within the physiological range, but rather indicated osteoblasts activation. Moreover, those new bones had a trabecular architecture that incorporated the glass particles within the bone structure. In fact, Sr substitution had been proven to promote mesenchymal cell differentiation and osteoblast proliferation as well as bone formation (Caetano-Lopes et al., 2007). Therefore, the effect of 0.1Sr W% therapy did not permanently inhibit the recovered physiological rises in bone forming activity, shortly following the cessation of antiresorptive treatment. Furthermore, it was unsurprising that the experimental dose of 0.1% Sr similar to that found in natural bone stimulated a rapid matrix synthesis. However, BG-Sr group showed significant difference in Oc.S/BS when compared to BG group; this finding corroborated the results indicating that Sr inhibits peptide osteoclasts (Yang et al., 2009). Moreover, osteoclasts contributed to limited biodegradation process and the results of osteoclast behavior presented here, were supported by the *in vivo* findings on cellulose-glass composites (Granito et al., 2010). The glass in those experiments was decomposed into granules to increase bone formation. After surgery, cellulose was surrounded by multinuclear giant cell fragments without association of glass particles. That limited number of osteoclasts proves that degradation of both bioactive glasses occured by non osteoclastic activity. The data suggested that the degradation mechanism of the biomaterial was likely to be due to chemical dissolution and that the role of osteoclasts was only minor.

Moreover, from those finding , the consistent bioactivity of the two biogactive glasses were largely the result of the uniformity of granules with a narrow range of 40 to 63 µm that had beneficial

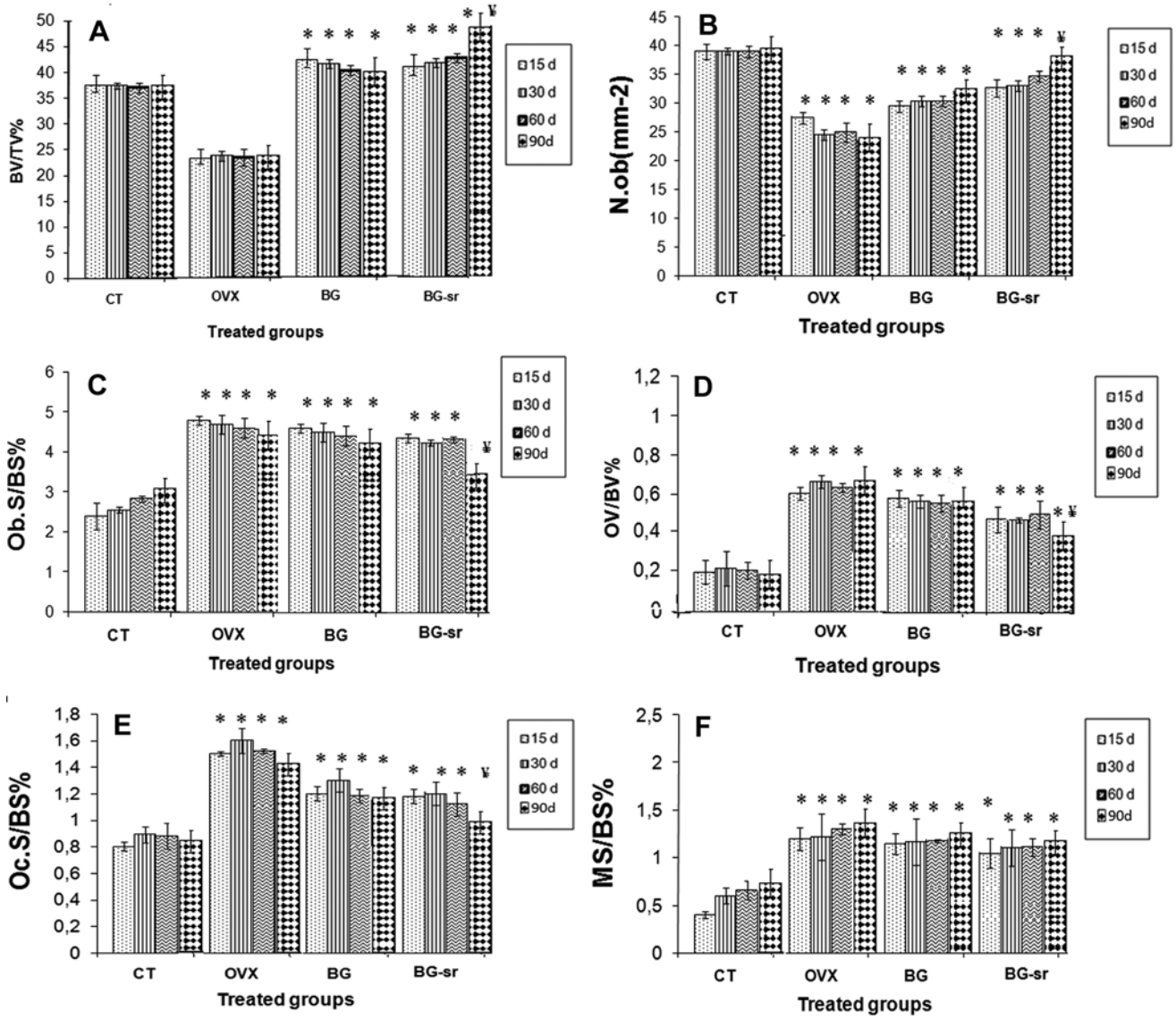

Fig. 5 Determination of (BV/TV) (A), (OV/BV) (B), (N.Ob) (C), (Oc.S/BS) (D), (MS/BS) (E) and (Ob.S/BS) (F) after 15, 30, 60, and 90 days in control femoral condyle Wistar rats (CT), ovariectomised (OVX) and filled with bioactive glass and strontium doped bioactive glass (BG and BG-Sr) * significantly higher activity in the indicated group than CT and OVX groups. # no significantly higher activity in the indicated group than group implanted with bioactive glass (BG).

effects on the bone regenerative capacity. It has been shown that when particle size was less than 200 μm, resorption occured rapidly (Gorustovich et al., 2007). Conversely, when particle size is greater than 400 μm, particles remained unreacted and were not resorbed, therefore; impeding the formation of new bone tissue throughout the particle-bone matrix (Li et al., 2007). It is plausible, therefore, that the gathering of all these properties such as particle size range, ionic dissolution products, ability to bond to hard tissue and to form a CHA layer present the keys to improve bone quality in the context of tissue engineering applications.

This study reveals that 0.1% of Sr in melting bioactive glass was shown to increase bone formation and ameliorate bonding to the bone. Furthermore, that study validates that bone mineral undergoes a maturation process. This rapid formation of CHA on BG-Sr surface indicates the high bioactivity of these biomaterials. Moreover, osteoproductive properties are evidenced for both biomaterials analyzed in this study. BG-Sr enhances bone formation and osteoblast recruitment when compared with BG. The histomorphometric and physicochemical measures of the implanted bone status, in ovariectomized rats hope that BG-Sr represents a promising biomaterial for bone regeneration in patients suffering from osteoporosis.

References

Barth A and Zscherp C (2002) What vibrations tell us about proteins. *Q Rev Biophys* **4**, 369–430.

Bohner M and Lemaitre J (2009) Can bioactivity be tested in vitro with SBF solution?. *Biomaterials* **30**, 2175–9.

Caetano-Lopes J, Canhão H, and Fonseca JE (2007) Osteoblasts and Bone Formation. *Acta Reumatol Port* 32, 103–10.

Danilchenko SN, Kukharenko OG, Moseke C, Protsenko IYu , Sukhodub LF, and Sulkio-Cleff B (2002) Determination of the bone mineral crystallite size and lattice strain from diffraction line broadening. *Cryst Res Technol* **37**, 1234–40.

De Carmejane O, Morris MD, Davis MK, and Stixrude L (2005) Bone Chemical Structure Response to Mechanical Stress Studied by High Pressure Raman Spectroscopy. *Calcif Tissue Int* **76**, 207–13.

Da Cruz AC, Pochapski MT, andTramonti R (2008) Evaluation of physical-chemical properties and biocompatibility of a microrough and smooth bioactive glass particles. *J Mater Sci-Mater M* **19**, 2809–17.

Furusawa T, Mizunuma K, Yamashita S, and Takahashi T (1998) Investigation of Early Bone Formation Using Resorbable Bioactive Glass in the Rat Mandible. *Int J Oral Max Impl* **13**, 672–6.

Furusawa T and Mizunuma K (1997) Osteoconductive properties and efficacy of resorbable bioactive glass as a bone grafting material. *Implant Dent* **6**, 93–101.

Gorustovich AA, Sivak MG, and Guglielmotti MB (2007) A novel methodology for imaging new bone formation around bioceramic bone substitutes. *J Biomed Mater Res A* **8**, 443–5.

Gorustovich AA, Steimetz T, Cabrini RL, and Porto López JM (2010) Osteoconductivity of strontium-doped bioactive glass particles: A histomorphometric study in rats. *J Biomed Mater Res A* **92**, 232–7.

Granito R N, Rennó AC, and Ravagnani C (2010) In vivo biological performance of a novel highly bioactive glass-ceramic (BiosilicateVR): A biomechanical and histomorphometric study in rat tibial defects. *J Biomed Mater Res B* **97**, 139–47.

Hench LL(1998) *Bioceramics J Am Ceram Soc* **81**, 1705–28.

Isaac J, Nohra J, Lao J, Jallot E, Nedelec JM, Berdal A et al. (2011) Effects of strontium-doped bioactive glass on the differentiation of cultured osteogenic cells. *Eur Cells Mater* **21**, 130–43.

Jallot E, Benhayoune H, Kilian L, Irigaray JL, Balossier G, and Bonhomme P (2000) Growth and dissolution of apatite precipitates formed in vivo on the surface of a bioactive glass coating film and its relevance to bioactivity. *J Phys D Appl Phys* **33**, 2775–80.

Jebahi S, Oudadesse H, El Feki H, Rebai T, Keskes H, Pellen P et al. (2012) Antioxidative/oxidative effects of strontium-doped bioactive glass as bone graft. in vivo assays in castrated rats. *J Appl Biomed* 10: 195–209.

Kokubo T and Takadama H (2006) How useful is SBF in predicting in vivo bone bioactivity?. *Biomaterials* **27**, 2907–15.

Lakhkar N, Abou Ne el EA, Salih V, and Knowles JC (2011)Titanium and Strontium-doped Phosphate Glasses as Vehicles for Strontium Ion Delivery to cells. *J Biomater Appl* **25**, 877–93.

Li ZY, Lam WM, and Yang C (2007) Chemical composition, crystal size and lattice structural changes after incorporation of strontium into biomimetic apatite. *Biomaterials* **28**, 1452–60.

Lochman P, Páral J, and Koèí J (2011) Gentamicin bound to the nanofibre microdispersed oxidized cellulose in the treatment of deep surgical site infections. *J Appl Biomed* **9**, 143–9.

Lusvardi G, Malavasi G, and Menabue L (2008) Properties of zinc releasing surfaces for clinical applications. *J Appl Biomed* **22**, 505–26.

Nguyen MC, Bui HT, Dang HH, Pham QL, Eun-Mi C, and Young HK (2010) Synthesis and anti-osteoporosis potential of two new indirubin-3-oxime derivatives. *J Korean Soc App Biol Chem* **53**, 22–6.

Oudadesse H, Dietrich E, Bui XV, Le Gal Y, Pellen P, and Cathelineau G (2011) Enhancement of cells proliferation and control of bioactivity of Strontium doped glass. *Appl Surf Sci* **257**, 8587–93.

Oudadesse H, Dietrich E, and Le Gal Y (2011) Apatite forming ability and cytocompatibility of pure and Zn-doped bioactive glasses. Biomed Mater.**6**, 035006.

Pan HB, Zhao XL, and Zhang X (2010) Strontium borate glass: potential biomaterial for bone regeneration. *J R Soc Interface* **7**, 1025–103.

Park YS, Park HJ, and Lee J (2012) Stabilization of glabridin by chitosan nano-complex. *J Korean Soc App Biol Chem* **55**, 457–62.

Schenk RK, Merz WA, and Müller JA (1969) quantitative histological study on bone resorption in human cancellous bone. *Acta Anat* **74**, 44–53.

Wahl DA and Czernuszka JT (2006) Collagen-hydroxyapatite composites for hard tissue repair. *Eur Cells Mater* **11**, 43–56.

Wiesmann HP, Meyer U, Plate U, and Höhling HJ (2004) Aspects of Collagen Mineralization in Hard Tissue Formation. *Int Rev Cytol* **242**, 121–56.

Yang F, Yang D, Tu J, Zheng Q, Cai L, and Wang L (2011) Strontium Enhances Osteogenic Differentiation of Mesenchymal Stem Cells and In vivo Bone Formation by Activating Wnt/Catenin Signaling. *Stem Cells* **29** 981–91.

Zhang X, Jia W, and Gu Y (2010) Teicoplanin-loaded borate bioactive glass implants for treating chronic boneinfection in a rabbit tibia osteomyelitis model. *Biomaterials* **31**, 5865–74.

Zhu LL, Zaidi S, Peng Y, Zhou H, Moonga BS and Blesius A (2007) Induction of a program gene expression during osteoblast differentiation with strontium ranelate. *Biochem Biophys Res Commun* **355**, 307–11.